

KINETIC MONTE CARLO SIMULATIONS OF ROD EUTECTICS AND THE SURFACE ROUGHENING TRANSITION IN BINARY ALLOYS

Daniel N. Bentz, William Betush, and Kenneth A. Jackson*

Materials Science and Engineering, University of Arizona

Abstract

In this paper we report on two related topics: Kinetic Monte Carlo simulations of the steady state growth of rod eutectics from the melt, and a study of the surface roughness of binary alloys.

We have implemented a three dimensional kinetic Monte Carlo (kMC) simulation with diffusion by pair exchange only in the liquid phase. Entropies of fusion are first chosen to fit the surface roughness of the pure materials, and the bond energies are derived from the equilibrium phase diagram, by treating the solid and liquid as regular and ideal solutions respectively. A simple cubic lattice oriented in the $\{100\}$ direction is used. Growth of the rods is initiated from columns of pure B material embedded in an A matrix, arranged in a close packed array with semi-periodic boundary conditions. The simulation cells typically have dimensions of 50 by 87 by 200 unit cells. Steady state growth is compliant with the Jackson-Hunt model. In the kMC simulations, using the spin-one Ising model, growth of each phase is faceted or non-faceted phases depending on the entropy of fusion.

There have been many studies of the surface roughening transition in single component systems, but none for binary alloy systems. The location of the surface roughening transition for the phases of a eutectic alloy determines whether the eutectic morphology will be regular or irregular. We have conducted a study of surface roughness on the spin-one Ising Model with diffusion using kMC. The surface roughness was found to scale with the melting temperature of the alloy as given by the liquidus line on the equilibrium phase diagram. The density of missing lateral bonds at the surface was used as a measure of surface roughness.

Introduction

The goal of this project is to gain insight into the kinetics of growth in faceted / non-faceted rod eutectic (irregular eutectic) alloys. These eutectic alloys often form irregular microstructures. For example, controlling the microstructure uniformity in irregular eutectics such as Ge-TiGe₂ and Si-TaSi₂ is critical in controlling their structural and electronic properties. Regular eutectics, where both phases are non-faceted, closely follow the Jackson-Hunt model,^{1,2} whereas irregular eutectics usually grow with a larger inter-phase spacing than predicted. This behavior is highlighted with the discrepancies reported between ground based and micro-gravity measurements.^{3,4}

Irregular eutectics have previously been modeled using adaptations of the Jackson-Hunt model⁵⁻⁷, however these analytical models do not address the nucleation of new atomic layers on the faceted phase. We have conducted kinetic Monte Carlo simulations (kMC) of eutectic growth based on the spin-one

Keywords: rod eutectics, eutectic growth, kinetic Monte Carlo, surface roughing, spin-one Ising model, theoretical

* Corresponding author. e-mail: kaj@aml.arizona.edu

Ising model, which provides a definitive description of the solid-liquid interface above and below the surface roughening transition⁸. This model will be used to gain insight into the growth kinetics of systems comprised of both faceted and non-faceted solid phases.

The second part of this report examines the interface roughness of a binary alloy. Since regular and irregular eutectics are classified by the surface roughness of the solid phases, understanding the surface roughening behavior is important. The location of the surface roughening transition for the two phases of a eutectic alloy determines whether the eutectic morphology will be regular or irregular. Below the roughening transition, there is nucleation barrier to the formation of new layers exists, and the growth rate depends on the kink site density.^{9,10} As a result, the undercooling required for growth on smooth interfaces below the transition point is much greater than for interfaces above the surface roughening transition, so the two behave quite differently.

Kinetic Monte Carlo

Simulations for this study were conducted using a spin-one Ising model with the liquid assumed to be an ideal solution in contact with a regular solution solid, where both phases are comprised of A and B atoms. Simulations are implemented on an initially flat solid-liquid interface. Solid atoms are added to the solid from the liquid at a rate of:

$$v_i^{LS} = v_o \exp\left(\frac{\Delta S_i}{k_B}\right) \quad (1)$$

Here ΔS_i is the entropy difference between the liquid and the solid phases of the A and B atoms, v_o is the pre-exponential factor with units of 1/time, and k_B is the Boltzmann's constant. Correspondingly, atoms leave the solid and join the liquid at a rate of:

$$v_i^{SL} = v_o \exp\left(-\sum_j \frac{\Phi_{ij}}{k_B T}\right) \quad (2)$$

Here Φ_{ij} represents A-A, B-B, and A-B bonds in the solid and T is the temperature of the system. Both solid-liquid bonds and liquid-liquid bonds energies are set to zero. Simulations reported for this study are all done isothermally. The number of both A and B atoms was conserved in the simulation cell. Diffusion was conducted only in the liquid and was implemented by pair exchange of B atoms at a rate proportional to add-atom arrival.

$$v_i^D = \vartheta v_i^{LS} = \frac{6D}{a} \quad (3)$$

where ϑ is the proportionality constant. This rate may also be written in terms of the diffusion coefficient D and the cube root of the atomic volume a.

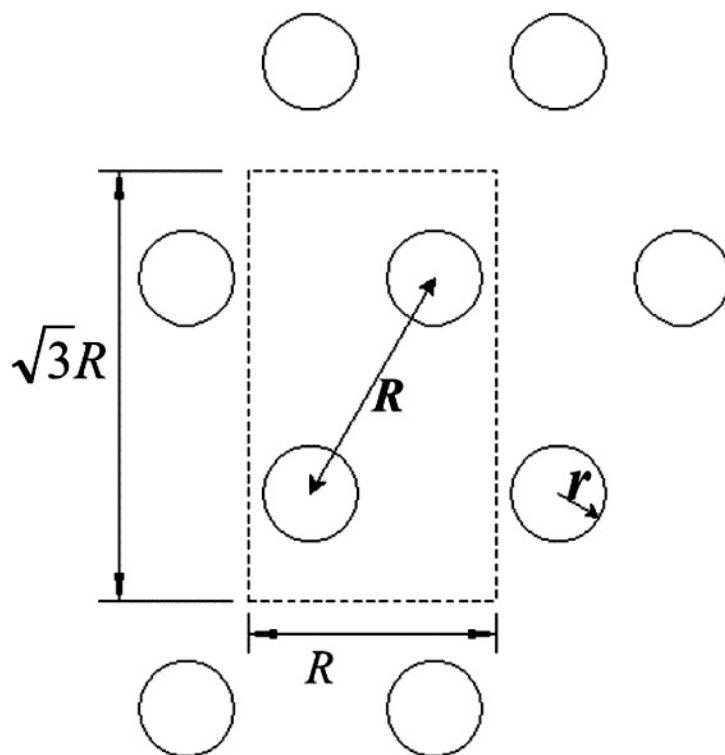


Figure 1. Simulation cell geometry.

Rods of solid B atoms are arranged in the simulation cell with semi-periodic boundary conditions in a closed packed formation. This is done with a simulation cell of R by $\sqrt{3}R$ where R is the rod spacing. The rod radius r is dependent on the eutectic composition.

These kMC simulations were implemented in a similar fashion to previous work,¹¹ events were chosen one at a time from a list of all possible events. The probability of choosing an event was inversely proportional to the frequency of that event. After the event is implemented the list is updated.

Rod Eutectic Simulations

The kMC simulations of a rod eutectic system started with a simulation cell where a liquid of randomly distributed A and B atoms was in contact with a solid consisting of columns of pure B embedded in an A matrix. The rods were arranged in a close packed formation in the simulation cell with periodic boundary conditions normal to the growth direction, as displayed in figure 1. The rod positions and radii are not confined in the simulation cell, however the simulation cell does place an upper limit on the rod spacing. Thus, the size of the simulation cell is an important parameter in these simulations.

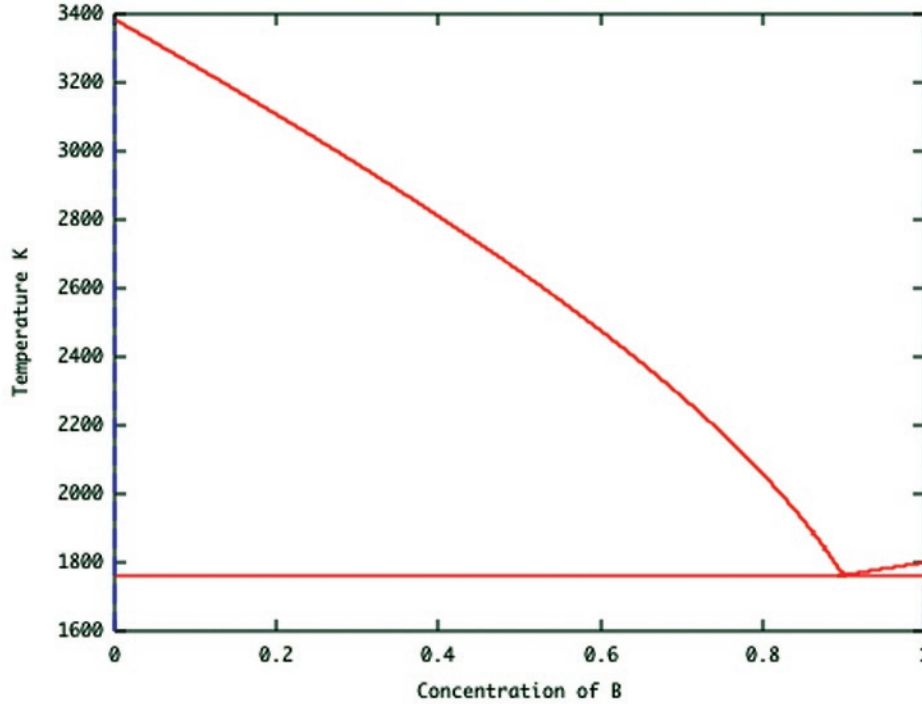


Figure 2. Sample phase diagram.

In the binary eutectic systems studied, the α and β phases contained very little of the second component.

The solidus lines in the phase diagram above are indistinguishable from the axis. This phase diagram was derived from the following bond energies:

$$\Phi_{AA} / k_B = 2820 \text{ }^\circ\text{K}, \Delta S_A = 2.5 k_B, \Phi_{BB} / k_B = 3000 \text{ }^\circ\text{K}, \Delta S_B = 5.0 k_B, \Phi_{AB} / k_B = 500 \text{ }^\circ\text{K}$$

Phase Diagram

Equilibrium phase diagrams for our eutectic systems were calculated for an ideal liquid in contact with a regular solution solid. In order to examine rod eutectic systems we used phase diagrams where the eutectic composition of the minor component was at 10%. The α and β phases in the eutectic systems used in this study contained very little of the second component.

Jackson-Hunt model

Starting values for the rod spacing R , which depends on the diffusion coefficient D and the simulation temperature, were derived from the Jackson-Hunt modeled. The temperature of the simulation, $T = T_E - \Delta T$, was chosen for reasonable rod spacing:

$$\Delta T \cdot R = C_1 (\Phi_{ij}, T_E, C_E, m_\alpha, m_\beta) \quad (4)$$

Where T_E and C_E are the eutectic temperature and composition and m_α and m_β are the slopes of the liquidus lines of the α and β phases at the eutectic point. Rod spacing R of ~ 90 unit cells were chosen based on computational restraints.

The rod spacing is related to the diffusion coefficient (D) by:

$$R^2 \cdot D = C_2 (T_E, C_E, \Delta S_\beta) \quad (5)$$

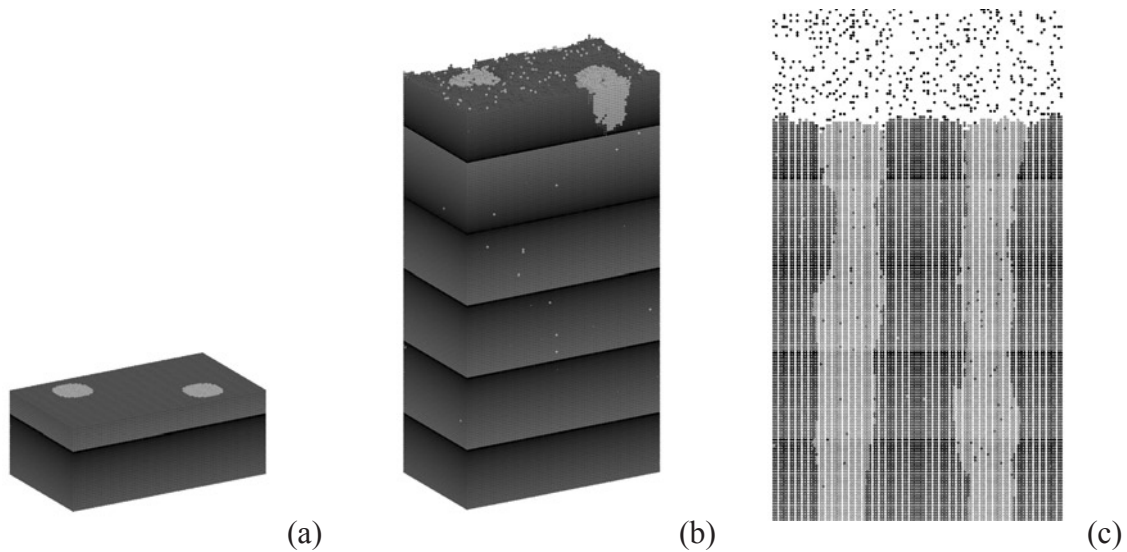


Figure 3. Typical simulation results.

(a) and (b) are 3D perspective views of the solid atoms in the simulation cell. (c) is a diagonal slice through the simulation cell of figure (b) where A and B solid atoms and B liquid atoms are displayed.

The simulation cell has dimensions of 50 by 87 by 230 unit-cells. Figures were rendered using Raster3D.¹²

$$\Phi_{AA} / k_B = 2820 \text{ }^\circ\text{K}, \Delta S_A = 2.5 k_B, \Phi_{BB} / k_B = 3000 \text{ }^\circ\text{K}, \Delta S_B = 5.0 k_B, \Phi_{AB} / k_B = 500 \text{ }^\circ\text{K}$$

$$T_E = 1762.6 \text{ }^\circ\text{K}, \Delta T = 68 \text{ }^\circ\text{K}$$

Results

Simulations of stable growing rod eutectics were based on a simple cubic lattice oriented in the $\{100\}$ growth direction. Stable rod growth was achieved when the liquid was 3% richer in the minor component as compared to the equilibrium phase diagram. The rods were also observed to modulate in thickness when the liquid was off this composition. Both of these behaviors are experimentally observed characteristics. An example of one of these simulations is displayed in figure 3.

Irregular Eutectics

Interest in examining the roughening behavior of the binary alloy was motivated by the simulation above. With a simple cubic simulation cell oriented in the $\{111\}$ direction and both A and B atoms having the same ΔS 's, we observed the surface roughness of the two phases was clearly different. The minor phase clearly showed faceting while the interface of the major phase was rough. We also observed that it was more difficult to get stable growth of faceted rods if the facets were in the plane of the growth direction. At this point we changed our focus from SC to FCC lattices since the SC $\{111\}$ simulation cell does not tessellate in the same way as the SC $\{100\}$ simulation cell. Since FCC $\{111\}$ planes have more in the plane nearest neighbors than $\{100\}$ direction systems may be rough $\{100\}$ faces while facets in the $\{111\}$ direction.

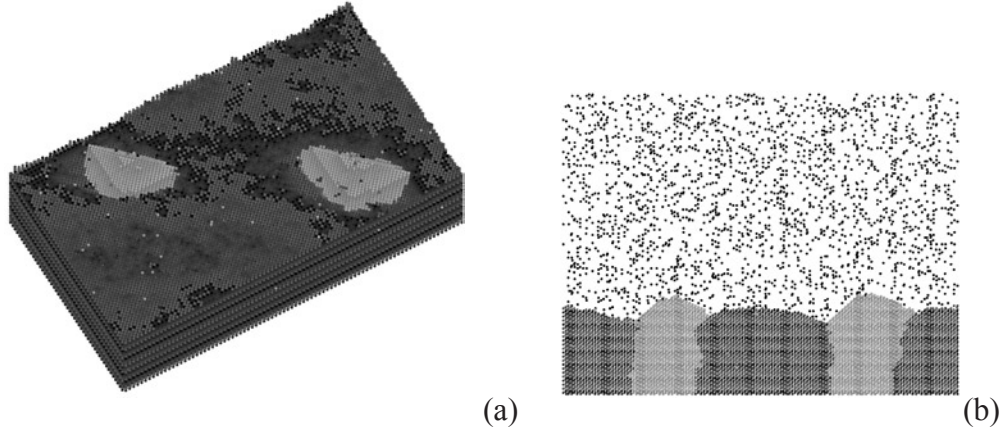


Figure 4. Irregular rod eutectic.

Simulation conducted on a simple cubic lattice oriented in the $\{111\}$ growth direction. Both A and B atoms gave the same ΔS however the surface roughness characteristics of both the alpha and beta phase are clearly different. Faceting is along of the $\{100\}$ faces. The 3D perspective view of figure (a) is distorted into a rectangular simulation cell. Figure (c) is a diagonal slice through the simulation cell.

$$\Phi_{AA} / k_B = 2000 \text{ }^\circ\text{K}, \Delta S_A = 5.0 k_B, \Phi_{BB} / k_B = 1650 \text{ }^\circ\text{K}, \Delta S_B = 5.0 k_B, \Phi_{AB} / k_B = 300 \text{ }^\circ\text{K}$$

$$T_E = 1028.2 \text{ }^\circ\text{K}, \Delta T = 9.2 \text{ }^\circ\text{K}$$

Surface Roughness

While the surface roughening transition of single component systems has been studied,¹³⁻¹⁵ the surface roughening transition for binary systems has not. We have conducted a study of the inter-facial roughness in alloys using the spin-one Ising Model with diffusion using kMC to understand the roughening behavior of the individual phases in the rod eutectic system. We have found that the surface roughness depends on the bond energies and melting temperature as given by the liquidus temperature on the equilibrium phase diagram.

The surface roughness can be defined in terms of the density of lateral bonds missing at the surface. In this study, the definition of surface roughness which was used is the same as used in BCF¹⁶:

$$s(t) = \frac{N_{SL}(t) - N_{SL}(0)}{N_{SL}(0)} \quad (6)$$

Here $N_{SL}(t)$ is the number of solid-liquid bonds on the surface and $N_{SL}(0)$ is the number of solid-liquid bonds on an atomically smooth surface. This does not define the location of the surface roughening transition, since the surface roughness increases smoothly through the transition. However, the location of the surface roughening transition can be determined from height-height correlations in the configurations of the interface.

For melt growth of single component materials, the location of the surface roughening transition is given by the Jackson α -factor.

$$\alpha = \left(\frac{L}{k_B T_m} \right) \left(\frac{\eta}{Z} \right) \quad (7)$$

Here L is the latent heat of fusion, T_m is the melting temperature of the system, η is the number of bonds in the plane of the interface, and Z is the coordination number of the lattice.

Surface Roughness Simulations

The relationship between surface roughness and the α -factor was examined on a FCC lattice oriented in the $\{100\}$ direction. Simulation cells typically had dimensions of 200 by 200 by 100 unit cells. Solid-liquid interfaces were created flat with pure solid of A atoms and a mixture of A and B atoms in the liquid. The evolution of structure of the interface then proceeded at the liquidus temperature of the binary alloy.

Surface Roughness Results

Three separate phase diagrams using different entropies of fusion for the pure α phase were used in the simulations reported here. System 1 was run with a ΔS of $7.0 k_B$, system 2 with a ΔS of $6.0 k_B$ and system 3 with a ΔS of $5.0 k_B$. Pure systems were also simulated over a similar range of α -factor values. Surface roughness as a function of α -factor values is reported in figure 5. Rather than using the melting point of the pure material to calculate the α -factor for the alloys, the liquidus temperature of the binary systems was used. Error bars on the data are the standard deviation of the fluctuations of the roughness value around the reported mean. Different α -factors values apply for each point along the liquidus lines of each phase diagram. From figure 5 it is evident that both pure and binary systems follow the same roughness relationship with a smooth monotonically decreasing roughness with increasing α -factor.

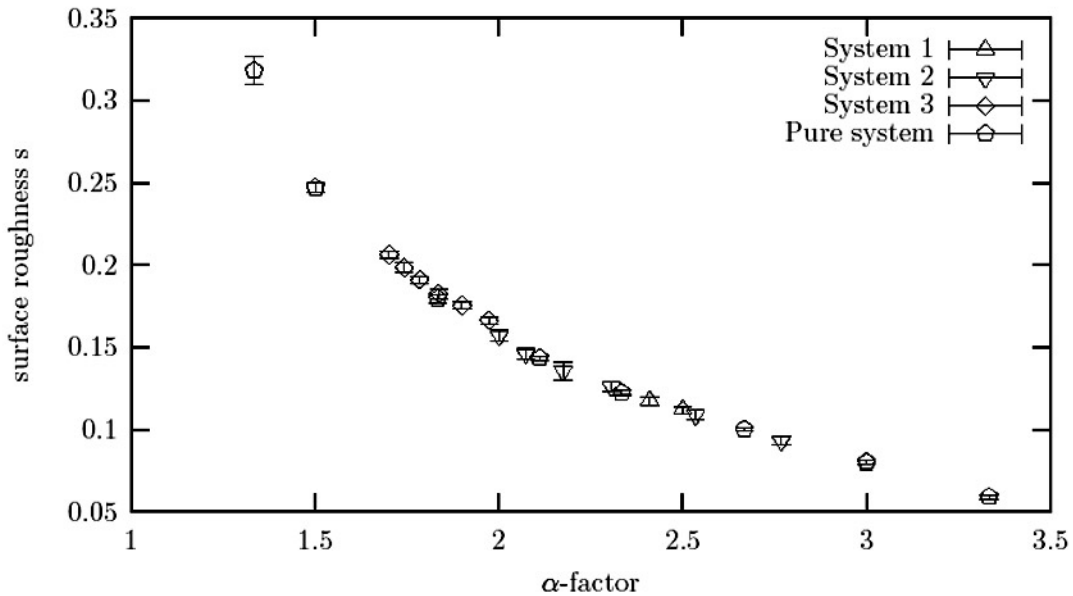


Figure 5. α -factor vs. roughness parameter

Both binary and pure systems follow the same roughness relationship

- System 1: $\Delta S_{\text{both}} = 7.0 k_B$, $\Phi_{AA} = 1500 \text{ } ^\circ\text{K}$, $\Phi_{BB} = 2000 \text{ } ^\circ\text{K}$, $\Phi_{AB} = 500 \text{ } ^\circ\text{K}$
- System 2: $\Delta S_{\text{both}} = 6.0 k_B$, $\Phi_{AA} = 1470 \text{ } ^\circ\text{K}$, $\Phi_{BB} = 2000 \text{ } ^\circ\text{K}$, $\Phi_{AB} = 500 \text{ } ^\circ\text{K}$
- System 3: $\Delta S_{\text{both}} = 5.0 k_B$, $\Phi_{AA} = 1310 \text{ } ^\circ\text{K}$, $\Phi_{BB} = 1800 \text{ } ^\circ\text{K}$, $\Phi_{AB} = 500 \text{ } ^\circ\text{K}$

In the case of this simple eutectic system the surface roughness of both phases increases as the system moves to either side of the eutectic. In a rod eutectic system this is more dramatic for the minor phase because of the larger difference between the melting temperature of the pure material and the alloy.

Conclusions

We have developed and demonstrated a kMC spin one Ising model capable of simulating the growth of stable rod eutectics. The simulations use the Jackson-Hunt model as a guide to provide appropriate starting conditions. These simulations exhibit behaviors similar to experimentally observed eutectic structures. While irregular rod eutectic growth has been more challenging, simulations where the minor phase is faceted have been more successful when the faceted interface has been out of the plane of the growth direction. Since the surface roughness of the two solid phases plays an important role in the development of the microstructure, an investigation of the surface roughness of binary alloys was conducted. It was found that the surface roughness of alloys follows the same behavior as pure materials provide that the liquidus temperature is used to calculate the α -factor. The entropy difference between pure solid and pure liquid of the same material is not the same as the entropy difference between the solid and the liquid alloy, and this difference is expressed in terms of the lowered melting point. The surface roughening of a phase in a eutectic alloy does not depend on the entropy of fusion of the pure components: the interfaces of the alloy are smoother than the interfaces of the pure materials.

Acknowledgments

NASA supported the work presented in this report through grant number NAG8-1667.

References

1. Jackson, K.A., and Hunt, J.D. "Lamellar and Rod Eutectic Growth." Transactions of the Metallurgical Society of Aime, vol. 236, no. 6, 1129-1142 (1966).
2. Hunt, J.D. and Jackson, K.A. "Binary Eutectic Solidification." Transactions of the Metallurgical Society of Aime, vol. 236, no. 6, 843-852 (1966).
3. Pirich, R.G., and Larson, D.J. "Influence of Gravity Driven Convection on the Directional Solidification of Bi/MnBi Eutectic Composites." Materials Processing in Reduced Gravity Environment of Space, G.E. Rindone, Ed., North Holland, New York, 523-531 (1982).
4. Pirich, R.G. "Gravitationally Induced Convection During Directional Solidification of Off-Eutectic Mn-Bi Alloys." Materials Processing in Reduced Gravity Environment of Space, G.E. Rindone, Ed., North Holland, New York, 593-602 (1982).
5. Fisher, D.J., and Kurz, W. "A Theory of Branching Limited Growth of Irregular Eutectics." Acta Metallurgica, vol. 28, no. 6, 777-794 (1980).
6. Magnin, P., Mason, J.T., and Trivedi, R. "Growth of Irregular Eutectics and the Al-Si System." Acta Metallurgica et Materialia, vol. 39, no. 4, 469-480 (1991).
7. Wolczynski, W. "Thermodynamics of Irregular Eutectic Growth." Materials Science Forum, vol. 215-216, 303-312 (1996).
8. Gilmer, G.H., and Broughton, J.Q. "Computer modeling of mass transport along surfaces." Annual review of materials science. Vol.16. Annual Reviews Palo Alto CA USA, viii+573 (1986).
9. Leamy, H. J., and Jackson, K. A. "Roughness of the Crystal-Vapor Interface." Journal of Applied Physics, vol. 42, no. 5, 2121-2127 (1971).
10. Jackson, K.A. "The Present State of the Theory of Crystal Growth from the Melt." Journal of Crystal Growth, vol. 24/25, 130-136 (1974).

11. Bentz, D.N., and Jackson, K.A. "Kinetic Monte Carlo Simulations of Dislocation Etch-Pits." Proceedings of the Materials Research Society, Symposium P, P2.5 (2001).
12. Merritt, E. A., and Bacon, D. J. "Raster3D: Photorealistic molecular graphics." Macromolecular Crystallography, Pt B, Methods in Enzymology, vol. 277, 505-524 (1997).
13. Shugard, W.J, Weeks, J.D., and Gilmer, G.H. "Monte Carlo Test of Theories for the Planar Model, the F Model, and Related Systems." Physical Review Letters, vol. 41, no. 20, 1399-1402 (1978).
14. Enckevort, W.J.P., and Eerden, J.P. "Monte Carlo Simulation of a {111} Diamond Face Around the Roughening Transition." Journal of Crystal Growth, vol. 47, 501-508 (1979).
15. Woodraska, D.L., Jaszczak, J.A. "A Monte Carlo simulation method for {111} surfaces of silicon and other diamond-cubic materials." Surface Science, vol. 374, no. 1-3, 319-32 (1997).
16. Burton, W.K., Cabrera, N., and Frank, F.C. "The Growth of Crystals and the Equilibrium Structure of their Surfaces." Philosophical Transactions of the Royal Society of London, vol. 243, no. 866, 299-358 (1951).